

TEST OF AN X-RAY CAVITY USING DOUBLE-BUNCHES FROM THE LCLS Cu-Linac*

K.-J. Kim[†], L. Assoufid, R.R. Lindberg, X. Shi, D. Shu, Y. Shvyd'ko, M. White
 Argonne National Laboratory, Argonne, IL, USA
 F.-J. Decker, Z. Huang, G. Marcus, T. Raubenheimer, T.-F. Tan, D. Zhu
 SLAC National Accelerator Laboratory, Menlo Park, CA, USA

Abstract

We discuss a proposal to test the operation of an X-ray cavity consisting of Bragg reflectors. The test will constitute a major step demonstrating the feasibility of either an X-ray regenerative amplifier FEL or an X-ray FEL Oscillator. These cavity-based X-ray FELs will provide the full temporal coherence lacking in the SASE FELs. An X-ray cavity of rectangular path will be constructed around the first seven LCLS-II undulator units. The Cu-linac will produce a pair of electron bunches separated by the cavity-round-trip distance during each linac cycle. The X-ray pulse produced by the first bunch is deflected into the cavity and returns to the undulator where it is amplified due to the presence of the second bunch. The key challenges are: the precision of the cavity mechanical construction, the quality of the diamond crystals, and the electron beam stability. When the LCLS-II super-conducting linac becomes available, the cavity can then be used for high-repetition rate studies of the X-ray RAFEL and XFEL concepts.

INTRODUCTION

X-ray free electron lasers (XFELs) such as the LCLS [1], based on Self-Amplified Spontaneous Emission (SASE) [2], are capable of producing extremely bright, transversely coherent, ultra-short X-ray pulses suitable for the investigation of ultra-fast chemical and physical processes [3-5]. A characteristic feature of single-pass SASE FEL amplifiers, however, is poor longitudinal coherence.

Temporally-coherent FEL pulses can be obtained by storing and recirculating the output of an amplifier in an X-ray cavity so that the X-ray pulse can interact with the following fresh electron bunches over many passes. The X-ray cavity is formed by a set of narrow bandwidth diamond Bragg crystals, which provide high reflectivity and monochromatization. This is the concept behind the cavity-based X-ray FELs (CBXFELs) such as the X-ray free-electron laser oscillator (XFEL) [6] and the X-ray regenerative amplifier free-electron laser (XRAFEL) [7]. The superconducting technology adopted by LCLS-II and LCLS-II-HE [8], will be capable of producing a constant stream of electron bunches (rather than pulsed/burst mode) with repetition rates up to 1 MHz, making the prospect of the CBXFEL realistic. The XFEL relies on a low-loss cavity supporting a low-gain FEL, While RAFEL leverages a high-gain FEL interaction.

* Work supported by U.S. DOE, Office of Science, Office of BES, under Contract No. DE-AC02-06CH11357 (ANL) and DE-AC02-76SF00515 (SLAC)

[†] kwangje@anl.gov

The defining properties of the XFEL are the extremely narrow and stable spectral bandwidths that can be as small as a few meV [9]. These characteristics conspire to push the average brightness of an XFEL source ~ 4 orders of magnitude higher than that of SASE at LCLS-II/-HE, as shown in Fig. 1[10]. Indeed, the *ultrafine* spectral capabil-

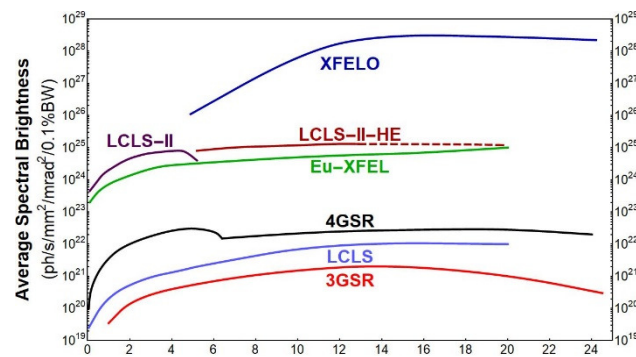


Figure 1: Brightness of various X-ray sources.

ities along with the high *spectral* photon density enabled by the XFEL would be complementary to the *ultrafast* temporal capabilities and high *temporal* photon density of the hard-X-ray SASE FELs. The scientific case for an XFEL is discussed in Ref. [11].

The XRAFEL concept, on the other hand, excels at bridging the gap between the performance characteristics of an HXR SASE FEL and an XFEL while directly addressing the science case that is targeted by the LCLS-II and LCLS-II-HE upgrades. The RAFEL system aims at the production of fully-longitudinally-coherent but shorter FEL pulses, and as such, has the unique ability to produce FEL X-ray pulses with both high *average* brightness and high *peak* brightness. The spectral output of a RAFEL is compared to SASE in Fig. 2.

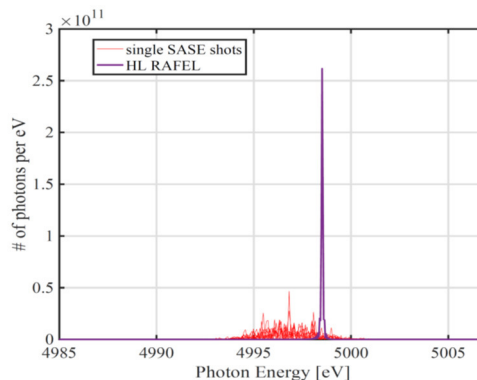


Figure 2: RAFEL and SASE.

Content from this work may be used under the terms of the CC BY 3.0 licence (© 2019). Any distribution of this work must maintain attribution to the author(s), title of the work, publisher, and DOI

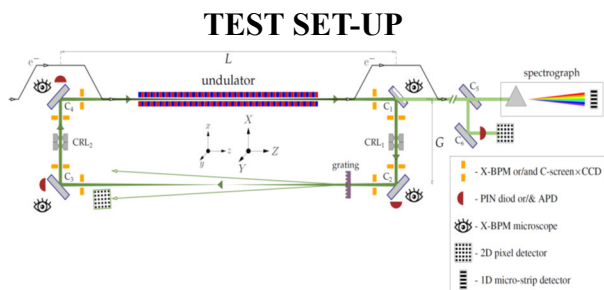


Figure 3: Set up for the X-ray cavity test.

R&D on some aspects of XFEL and RAFL has been on-going at ANL [12-13] and SLAC [14]. This proposal is to test the key aspect of a cavity-based XFEL—the operation of an X-ray cavity that can store an X-ray pulse produced by an electron bunch and that the pulse can be amplified by another electron bunch a rectangular X-ray cavity will be constructed around the first seven sections of the LSLS-II hard X-ray undulator, formed by four diamond crystals. The schematics of the test cavity is shown in Fig. 3. Note that the scales in the x - and z -directions are quite different. Various parameters for the test experiment, electron beam parameters such as the bunch charge Q , FWHM length τ , FWHM energy spread ΔE , RMS beam size σ_x , and RMS beam angular divergence $\sigma_{x'}$, as well as those for the undulator and cavity are shown in Table 1. Electron bunches possessing these parameters are used in regular LCLS operation and are well characterized.

Table 1: Major Parameters

E- bunch (XFEL, RAFL)	
E_e [GeV]	10.3
Q [pC]	100, 150
τ [fs]	300, 50
σ_x [μm]	22, 24
$\sigma_{x'}$ [μr]	1.1, 1.2
ΔE [MeV]	0.5, 1.5
Bunch spacing [m]	66
Undulator	
λ_u [cm]	2.8
N_u	130x7
K	2.44
L_u [m]	4x7=28
Cavity	
Crystal	C*(400)
Bragg angle θ	45°
$\hbar\omega$ [keV]	9.83
λ [Å]	1.26
$\Delta\hbar\omega$ [meV]	75
$\Delta\theta$ [μr]	8
L, G [m]	32, 1

The rectangular cavity configuration is chosen, rather than the tuneable, zig-zag path [15-16] due to the limitation in the available transverse space. Diamond crystals of (100) surface will be used, for which high quality samples

have been available from multiple vendors. The photon energy /wavelength are determined from the Bragg angle 45°. The reflection bandwidth in energy is 75 meV and 8 μr in angle. $K = 2.44$ is the maximum deflection parameter [17] and the corresponding electron energy is $E_e = 10.34$ GeV. If desired, a smaller value of K and a corresponding E_e may be employed. The SLAC Cu-linac produces a pair of bunches spaced by 66 m, the roundtrip distance of the X-ray cavity. A small portion of the circulating photons are peeled off for diagnostics, either through a thin crystal C_1 [18] or by a diamond grating [19-20].

PHOTON MEASUREMENTS

Low Gain for XFEL

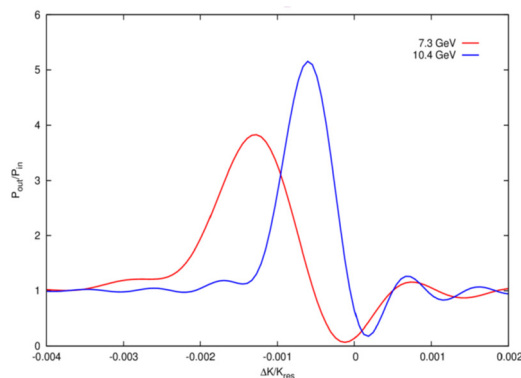


Figure 4: Gain in the XFEL mode.

The number of photons produced by the first bunch, monochromatized and deflected into the cavity, is $\Delta N_\gamma = 5.8 \times 10^4$. The maximum intensity gain computed by GINGER [21] is about 5, as shown in Fig. 4. The gain, however, occurs only to the cylindrically symmetric component of the radiation. For undulator radiation, the symmetric part is about 1/6 of the total intensity [22]. Therefore, the effective gain of the spectral intensity will be about a factor of two, which should be readily measurable.

High Gain for XRAFL

Time-independent simulations using the FEL code Genesis [23] suggest that the single-pass FEL gain within the cavity is > 150 (see Fig. 5). The radiation generated

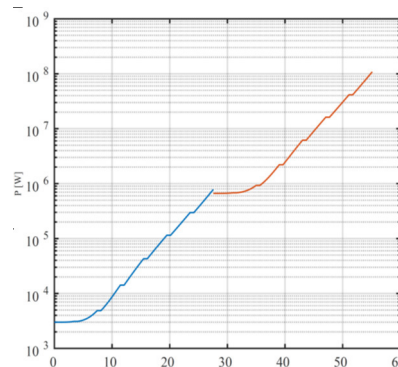


Figure 5: Two pass growth in RAFL mode.

in the first pass (blue curve in Fig. 5) is propagated through the optical cavity shown in Fig. 3 using custom built Fourier optics routines. Here, the cavity is assumed to be perfectly aligned and has an overall throughput efficiency of 85%. Time-dependent simulations including a cavity stability analysis in the presence of diamond angular errors are currently underway.

TOLERANCES

The tolerance specification is complicated, needing to take into account the pulse shape, time-scale, number of ensembles, etc. Here we will give simplistic estimates for the two most critical tolerances—on the angular placement of the Bragg crystals and the cavity roundtrip time.

Crystal Angle

We assume that the two CRL lenses are identical and that the Rayleigh length is 20 m, the same as the electron beam beta function, we find $f=20.4$ m for the one turn transfer matrix to be stable. We will specify the tolerances for the crystal mirrors such that the trajectory deviation of the X-rays after one turn is smaller than one third of the RMS beam size. Then we find that the angular tolerances to be less than 80 nr. In this exercise, the angular error in each mirror is random and independent. This may be an optimistic assumption since there are only four crystals involved. We therefore set the angular tolerance twice tighter, to 40 nr.

The tolerances are relaxed for RAFEL due to the optical guiding in a high-gain amplification. Simulation results indicate that the tolerances can be relaxed by a factor of three.

Roundtrip Time

The jitter in the roundtrip time of the cavity should be less than one tenth of the bunch length for XFEL. For XRA FEL the time tolerance may be relaxed by a factor of two. Thus, we specify the tolerance in time jitter for the case of XFEL at 30 fs, while it is 10 fs for XFEL.

MECHANICAL DESIGN OF THE X-RAY CAVITY

The diamond crystals will be operated with holders at stabilized temperature so that the instantaneous heat load due to the x-ray pulses does not degrade and shift the reflectivity profile. The crystal cooling system should be low-vibration and additionally, will require two-axis tip-tilting nanopositioning stages with nanoradian-scale positioning resolution and stability. A planar-shape, high-stiffness, high-precision weak-link structure developed at APS [24] has typical angular positioning resolution and stability of 5-50 nrad with a travel range of up to 1.2-degrees, and can be made ultra-high-vacuum (UHV)-compatible. Figure 6 shows a 3D model of the pitch and roll tip-tilting nanopositioning stages that will be applied for the x-ray cavity diamond crystal alignment. The diamond crystal holder and two miniature linear stages will be mounted on the top of the tip-tilting stages, which are not shown in the figure.

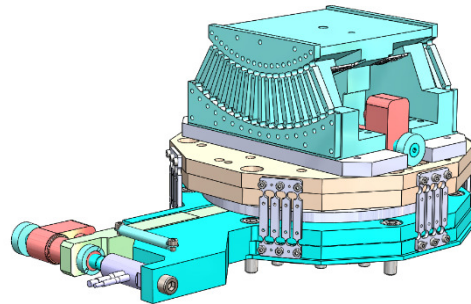


Figure 6: A 3D model of the Pitch and Roll nano-positioning stages for diamond crystal alignment.

ALIGNMENT STRATEGY

To help in alignment, eight X-ray beam position monitors (X-BPMs), two each near the two ends of the four straight paths, will be installed, as indicated in Fig.3. Aligning the X-ray cavity to the desired precision is a complex task, and can be accomplished by reducing the degree of freedom (DOF) step-by-step, beginning with an infinite-number-of-DOF problem to that of a-one-DOF problem. The steps are as follows:

- ∞ to 3D: Four crystal mirrors, two CRLs, and eight X-BPMs are put into nominal positions to a 20-30 μm accuracy using the laser interferometer system Etalon AMT.
- 3D to 2 D: The X-ray paths are forced into the nominal cavity plane by properly aligning roll/tilt angles of the diamond crystals.
- 2D to 1D: All multiply-reflected beams are forced to overlap by properly aligning crystal positions and pitch/Bragg angles.
- 1D: Adjust the round-trip cavity length by translating C1, C2, and CRL1 simultaneously along z (Fig. 3).

DISCUSSION

If the proposed experiment concludes successfully and the superconducting LCLS-II linac is in operation, the rectangular diamond cavity can be upgraded to a larger, non-coplanar but tuneable cavity [25] to develop full RAFEL/XFEL operation modes for LCLS-II. Another proposal to use the double bunch from the Cu-linac and a four-crystal monochromator for self-seeding to achieve high power X-ray pulses is described in Ref. [26] of this conference.

REFERENCES

- [1] P. Emma *et al.*, "First lasing and operation of angstrom-wavelength free electron laser," *Nature Photonics*, vol4, p. 461, 2007.
- [2] A. Kondratenko and E. Saldin, "Generation of coherent radiation by a relativistic electron beam in an undulator," *Part. Accelerators*, vol. 10, p. 207, 1980.

- Content from this work may be used under the terms of the CC BY 3.0 licence (© 2019). Any distribution of this work must maintain attribution to the author(s), title of the work, publisher, and DOI
- [3] R. Bonifacio, C. Pellegrini, and L. M. Narducci, "Collective instabilities and high-gain regime free electron laser," in *Free Electron Generation of Extreme Ultraviolet Coherent Radiation*, J. M. J. Madey and C. Pellegrini, Eds., no. 118. SPIE, p. 236, 1984.
- [4] Z. Huang and K.-J. Kim, "Review of X-ray free-electron laser theory," *Phys. Rev. ST-AB*, vol. 10, p. 034801, 2007.
- [5] K.-J. Kim, Z. Huang, and R. Lindberg, "Synchrotron Radiation and Free Electron Lasers: Principles of Coherent X-Ray Generation," Cambridge University Press, 2017.
- [6] K.-J. Kim, Y. Shvyd'ko, and S. Reiche, "A proposal for an X-ray free-electron laser with an energy-recovery linac," *Phys. Rev. Lett.*, vol. 100, p. 244802, 2008.
- [7] Z. Huang and R. D. Ruth, "Fully Coherent X-Ray Pulses from a Regenerative-Amplifier Free-Electron Laser," *PRL* **96**, 144801 (2006).
- [8] T. Raubenheimer, The LCLS-II-HE, A High Energy upgrade of the LCLS-II. 60th ICFA Advanced Beam Dynamics Workshop on Future Light Sources FLS2018, Shanghai, China, 2018.
- [9] R. R. Lindberg, K.-J. Kim, Y. Shvyd'ko, and W. M. Fawley, Performance of the X-ray free-electron laser with crystal Cavity, *Phys. Rev. ST Accel. Beams*. **14**, 010701 (2011).
- [10] W. Qin, et al., Start-to-end simulation for an X-ray FEL oscillator at the LCLS-II and LCLS II-HE, in *Proc. 2017 International FEL conf.* (2017).
- [11] B. Adams *et al.*, Scientific Opportunities with an X-ray Free-Electron Laser Oscillator, arXiv:1903.09317 [physics.ins-det].
- [12] K.-J. Kim *et al.*, "An oscillator configuration for full realization of hard x-ray free electron laser," in *Proc. 7th Int. Particle Accelerator Conf. (IPAC16)*, Busan, Korea, May 2016, pp. 801-804. doi:10.18429/JACoW-IPAC2016-MOPOW039
- [13] K.-J. Kim, "Free Electron Laser Oscillator—A New Type of X-ray Laser," in *Nonlinear Dynamics and Collective Effects in Particle Beam Physics*, p. 192, Proc. Of the NOCE 2017 Workshop, Arcidosso, Italy, September 19-22, 2017.
- [14] G. Marcus, *private communication*.
- [15] R. M. J. Cotterill, "A universal planar X-ray resonator," *Appl. Phys. Lett.*, vol. 12, p. 403, 1968.
- [16] K.-J. Kim and Y. Shvyd'ko, Tunable optical cavity for an x-ray free-electron-laser oscillator, *Phys. Rev. ST Accel. Beams*. **12**, 030703 (2009)
- [17] LCLS-II Undulator System, Physics requirement document #LCLSII-3.2-PR-0038-R2.
- [18] T. Kolodziej, P. Vodnala, S. Terentyev, V. Blank, and Yu. Shvyd'ko, *Journal of Applied Crystallography* **49** (2016) 1240.
- [19] K. Katayama, *et al.*, "A beam branching method for timing and spectral characterization of hard x-ray free electron lasers", *Structural Dynamics* **3**, 024301 (2016).
- [20] K. Li, M. Chollet, *et al.*, in preparation.
- [21] W. M. Fawley, "A user manual for GINGER and its post-processor XPLOTGIN," *LBL*, Report LBNL-49625, 2002
- [22] Y. S. Li, R.R. Lindberg, and K.-J. Kim, in preparation.
- [23] S. Reiche, "GENESIS 1.3: a fully 3D time-dependent FEL simulation code," *Nucl. Instrum. Methods Phys. Res., Sect. A*, vol. 429, p. 243, 1999.
- [24] U.S. Patent granted No. 6,984,335, D. Shu, T. S. Toellner, and E. E. Alp, 2006.
- [25] Yu. Shvyd'ko, *Beam Dynamics Newsletter* **60**, 68 (2013), International Committee for Future Accelerators.
- [26] A. Halavanau et al., "Generation of high-power hard x-rays at LCLS-II with double bunch self-seeding", presented at the 10th Int. Particle Accelerator Conf. (IPAC19), Melbourne, Australia, May 2019, paper TUPRB088, this conference.